A turbulent quarter century of active grids: From Makita (1991) to the present

A turbulent quarter century of active grids: From Makita (1991) to the present

Laurent Mydlarski

Department of Mechanical Engineering, McGill University, Montréal, Québec, CANADA

E-mail: laurent.mydlarski@mcgill.ca

December 31, 2016

Abstract. A quarter of a century ago, following a series of investigations with his colleagues, Makita published a paper [*Fluid Dyn. Res.*, **8**, 53-64, (1991)] in which the production of high-Reynolds-number, homogeneous, isotropic turbulence in a typical laboratory-sized wind tunnel by way of a novel "active grid" was demonstrated. Until this time, classical ("passive") grids had been used to generate homogeneous, isotropic turbulence, which was almost invariably of low Reynolds number. In the years following the publication of Makita's paper, active grids have played a major role in experimental studies of turbulence, given their ability to generate the most fundamental expression of a turbulent flow (homogeneous, isotropic turbulence) at Reynolds numbers large enough to i) test Kolmogorov theory (posed in the limit of infinite Reynolds numbers), and ii) match those of many natural and industrial flows. The present paper aims to review the research related to active grids undertaken since Makita's seminal work. To this end, it firstly summarizes the key elements involved in the design, construction and operation of active grids, with the aim of providing a useful reference for those interested in studying or building active grids. Secondly, it discusses how active grids are now being customized to generate novel flows. Lastly, it reviews the accomplishments that have been achieved as a result of the invention of the active grid. It is hoped that the contribution to the field of turbulence brought by active grids a quarter of a century ago will moreover serve to inspire current fluid dynamicists to generate other simple and elegant innovations – like the active grid – to further advance our understanding of turbulent flows.

Keywords: Active grids, homogeneous isotropic turbulence, high-Reynolds-number, wind tunnels

1. Introduction

Fluid dynamicists have been investigating turbulent flows since the pioneering work of Osborne Reynolds (Reynolds, 1883a,b), which opened the door to the beautiful, but challenging subject of turbulence over 130 years ago. Turbulent flows are often classified into various categories, many of which overlap – *e.g.*, isotropic or anisotropic flows, homogeneous or inhomogeneous ones, wall-bounded or free-shear flows (both categories of shear flows), *etc.* In all cases, however, the consensus amongst scientists and engineers studying turbulent flows for over a century is that turbulence is complex, given its chaotic nature that is intimately tied to the non-linear Navier-Stokes equations. To best study a such an abstruse phenomenon, it is therefore logical to examine its most simple expression, which is homogeneous, isotropic turbulence. In such a flow, the turbulent kinetic energy budget simplifies to (Tennekes and Lumley, 1972, Pope, 2000):

$$\frac{d}{dt}\langle\frac{1}{2}u_iu_i\rangle = -\epsilon, \tag{1}$$

where u_i is the fluctuating component of the velocity vector, and $\epsilon = 2\nu\langle s_{ij}s_{ij}\rangle$ is the dissipation rate of turbulent kinetic energy, with ν being the kinematic viscosity and $s_{ij} \equiv \frac{1}{2}(\frac{\partial u_i}{\partial x_j} + \frac{\partial u_j}{\partial x_i})$ being the fluctuating strain rate. Although difficult to exactly achieve in an experimental setting, the most readily (and therefore commonly) studied approximation to homogeneous, isotropic turbulence is grid-generated, wind-tunnel turbulence.‡ For over half a century, homogeneous, isotropic turbulence was almost universally generated in wind tunnels by placing a grid of horizontal and vertical bars at the upstream end of a wind-tunnel test section, generally downstream of a flow-conditioning section / contraction (Simmons and Salter, 1934, 1938, Stewart and Townsend, 1951, Comte-Bellot and Corrsin, 1966, 1971, Lavoie et al., 2007). Sufficiently far downstream of the grid ($x/M \gtrsim 20-30$, where M is the mesh length of the grid), the flow becomes effectively homogeneous and isotropic (Isaza et al., 2014), with the turbulence in the downstream direction decaying sufficiently slowly that equation (1) can be approximated as:

$$U\frac{\partial}{\partial x_1}\langle\frac{1}{2}u_iu_i\rangle = -\epsilon, \tag{2}$$

in a frame of reference that is fixed to the wind tunnel, where U is the mean velocity in the downstream (x_1) direction (and the x_2 and x_3 directions are those normal to the mean flow).

The quality of the turbulence generated in the above-described way is generally excellent. If i) the mesh length of the grid is substantially smaller than the wind tunnel width (W), and ii) measurements are made sufficiently far downstream ($x/M \gtrsim 20-30$), the resulting turbulent flow can exhibit a high degree of homogeneity in the core of the flow (*i.e.* sufficiently far away from the boundary layers that form on the

‡ Another approximation to homogeneous isotropic turbulence is that generated by way of one or more oscillating grids in an otherwise stationary fluid (*e.g.* De Silva and Fernando, 1994, Variano and Cowen, 2008). Such a flow has a nominally zero-mean velocity – a useful characteristic in certain contexts. However, it i) suffers from larger inhomogeneity in the direction normal to the oscillating grid than grid-generated wind-tunnel turbulence, and ii) has not been as extensively studied given the increased (historical) complexity in making measurements of velocity in flows with zero mean velocity. This latter limitation results from the fact that hot-wire anemometry was the dominant tool in the measurement of turbulence for decades and is, without non-trivial increases in complexity, incapable of accurately measuring velocity in flows with no mean velocity.

wind-tunnel walls). Moreover, the degree of isotropy of the flow can be quite high (*e.g.* $u_{rms}/v_{rms} \approx 1.1$), and can be further improved by the addition of a secondary contraction downstream of the grid (Comte-Bellot and Corrsin, 1966, Lavoie et al., 2007). However, grid turbulence generated in this way is, with a few, often impractical, exceptions (*e.g.* Kistler and Vrebalovich, 1966), characterized by low Reynolds numbers (typically $Re_\lambda \equiv u_{rms}\lambda/\nu \lesssim 10^2$, where λ is the Taylor microscale). This limitation is problematic given that i) the main underlying theory of turbulent flows (Kolmogorov theory, Kolmogorov (1941a,b)) is posed in the limit of infinite Reynolds numbers, and ii) the magnitude of the Reynolds numbers that characterize grid turbulence are below those of most industrial flows, and certainly much smaller than those of the atmospheric and oceanic flows that play critical roles in our daily lives, (*e.g.* weather forecasting, environmental pollutant dispersion).

For the above reasons, fluid dynamicists have attempted to generate high-Reynolds-number, homogeneous, isotropic turbulence within standard laboratory wind tunnels (*e.g.* Ling and Wan, 1972, Gad-el Hak and Corrsin, 1974, Tassa and Kamotani, 1975) using, for example, grids with oscillating agitator bars or grids with attached jets. Unfortunately, such attempts met with only moderate success. However, a major advance in generating homogeneous, isotropic wind tunnel turbulence was achieved by Makita and colleagues at the Toyohashi University of Technology in Japan, and best described in an article published a quarter-century ago (Makita, 1991). (See also Makita and Miyamoto (1983), Makita et al. (1987a,b), Makita, Iwasaki, Ida and Sassa (1988), Makita, Iida and Sassa (1988), Makita et al. (1989), Makita and Sassa (1991) for earlier conference proceedings and articles in Japanese.) Using a bi-planar "active" grid, Makita and co-workers were able to achieve a high-Reynolds-number flow ($Re_\lambda \approx 400$) in a wind tunnel of only 0.7×0.7 m^2 cross-section at a moderate speed of 5 m/s. Makita was able to achieve such a Reynolds number by i) attaching triangular agitator wings to the 15 horizontal and 15 vertical (6-mm-diameter) round grid bars, and ii) rotating the latter at a speed of 2 revolutions per second using stepper motors located outside of the wind tunnel, but independently and randomly changing their direction of rotation. Doing so increased both the flow's turbulent kinetic energy and its integral length scale (ℓ). The end result was a flow with a Taylor-microscale Reynolds number nearly an order of magnitude larger than what would have been achieved with a traditional grid of similar mesh length (M=46.7 mm) at the same mean flow velocity. This is all the more impressive when one recalls that an increase in Re_λ by an order of magnitude corresponds to an increase in $R_\ell (\equiv u_{rms}\ell/\nu)$ of two orders of magnitude (Tennekes and Lumley, 1972). Moreover, the resulting flow was shearless and exhibited i) a high degree of homogeneity, ii) probability density functions (PDFs) that were consistent with homogeneous, isotropic flow, and iii) well-developed spectra with inertial subranges that were over one decade wide in wavenumber space and of slopes approaching -5/3. The only downside was a slightly higher large-scale anisotropy (u_{rms}/v_{rms}) of 1.22 at $x/M = 100$.

Given the above success in generating high-Reynolds-number, quasi-homogeneous, isotropic turbulence in a standard laboratory-sized wind tunnel, the work of Makita and co-workers was well received by the fluid dynamics community. Warhaft and collaborators at Cornell University were the first to exploit Makita's design and build their own active grids (Mydlarski and Warhaft, 1996, 1998a), with other research groups doing the same thereafter. Active grids have now been used to achieve homogeneous, isotropic flows with Reynolds numbers as large as $Re_\lambda \sim 1.4 \times 10^4$ (Larssen and Devenport, 2011), and are therefore now commonplace, existing in fluid mechanics laboratories across the world. This is testified by the fact that the traditional grids used to generate wind-tunnel turbulence for over half a century are now regularly referred to as "passive grids," even when not being contrasted with active grids (*e.g.* Lavoie et al., 2007, Lee et al., 2014).§

Now that a quarter-century has passed since the publication of Makita's 1991 paper, which moreover coincides with the thirtieth anniversary of *Fluid Dynamics Research*, the journal in which Makita published his seminal work, it is both timely and appropriate to review active grids and the impact they have had on the study of turbulence. In this context, the present review paper has three objectives:

(i) to provide a summary of the key elements involved in the design, construction and operation of active grids, while compiling improvements and recommendations of others who have already built active grids, with the aim of providing a useful reference for those interested in active grids, including those explicitly intending to build one of their own,

(ii) to discuss how active grids are now being used to "customize" novel flows by tuning active grids, and

(iii) to review the accomplishments that have been achieved using active grids.

In the remainder of this paper, the above three topics will be respectively discussed in the subsequent three sections. A final section will provide concluding remarks.

2. Active grid design, construction and operation

As noted above, the first objective of this work is to review the design, construction and operation of active grids, with the intent of collating the experiences of previous builders of active grids in a way that will provide a useful reference on active grids. Doing so, however, will hopefully also result in secondary benefits, such as an increased appreciation of the effect of differences in various active grid designs and their methods of operation. To this end, the remainder of the section is divided into two subsections: the first treating the design and construction of active grids, and the second covering their operation.

§ It should, however, be noted that the term "passive grid" was employed well-before 1991, in the context of earlier attempts at active grids (*e.g.* Ling and Wan, 1972).

2.1. Active grid design and construction

The vast majority of active grids follow the general design of proposed by Makita (1991), briefly alluded to in §1. They consist of grid bars i) to which are attached "agitator wings," and ii) that are rotated by steppers motors located outside of the grid/tunnel. To give the reader a better idea of their general construction, figure 1 depicts a schematic of the original active grid developed by Makita and co-workers, as well as pictures of two other active grids.

Clearly, the overall dimensions of an active grid are dictated by the size and shape of the wind or water tunnel in which it is to be placed. A first important choice that an active grid designer must make is the mesh length, or, alternatively, the number of mesh lengths spanning the tunnel cross section (assuming that the tunnel cross-sectional area is predetermined). Active grids have been constructed with mesh lengths as small as 3.75 cm (Poorte and Biesheuvel, 2002) and as large as 21 cm (Larssen and Devenport, 2011). The number of mesh lengths have varied from 6 $\times$ 8 (Kang et al., 2003) to 20 $\times$ 20 (Michioka et al., 2011). As most active grids are designed with the intention of achieving as large of a Reynolds number as possible, one might be inclined to make M as large as possible, given that the integral length scale of the turbulence scales with M. However, as M, and therefore ℓ, increase, the ratio of the tunnel width to the integral length scale, W/ℓ, decreases. When this latter value becomes too small, the flow will cease to be homogeneous, as the flow can now "feel" the test section boundaries, at which the no-slip condition holds. Stated in another way, a flow in a wind or water tunnel can only be homogeneous in the limit $W/\ell \to \infty$. This effect can be observed when comparing the homogeneity plots of Makita (1991) (his figure 8) and those of Mydlarski and Warhaft (1996) (their figure 2), for which the data is complied in figure 2. In the work of Makita (1991), the active grid dimensions are $15M \times 15M$ and the flow consequently exhibits a larger homogeneous core than that of Mydlarski and Warhaft (1996), for which the active grid dimensions are $8M \times 8M$. (Note that the smaller extent of the homogeneous core is more pronounced in the RMS profiles.) In the end, it is ultimately a compromise between two competing effects, and the active grid builder must decide upon the balance between the degree of the flow's homogeneity and its Reynolds number. Of relevance to this issue is an observation of Larssen and Devenport (2011), who found that the flow generated by active grids was homogeneous at distances more than two integral length scales away from the wall. In any case, if homogeneity of the flow is a critical characteristic, then selecting $M \approx W/10$ would be a sensible rule of thumb for the upper-limit on an active grid mesh length, keeping in mind that under typical operating conditions, most active grids generate flows with $\ell/M > 1$, whereas passive grids generate flows in which $\ell/M < 1$ initially. Lastly, for researchers interested in turbulent mixing of passive scalars, it is worth noting that passive scalar fields advected by active-grid-generated turbulence seem particularly sensitive to the boundary effects that can arise when W is not substantially larger than ℓ. Mydlarski and Warhaft (1998a) noted that i) a mean scalar (temperature) gradient imposed upon

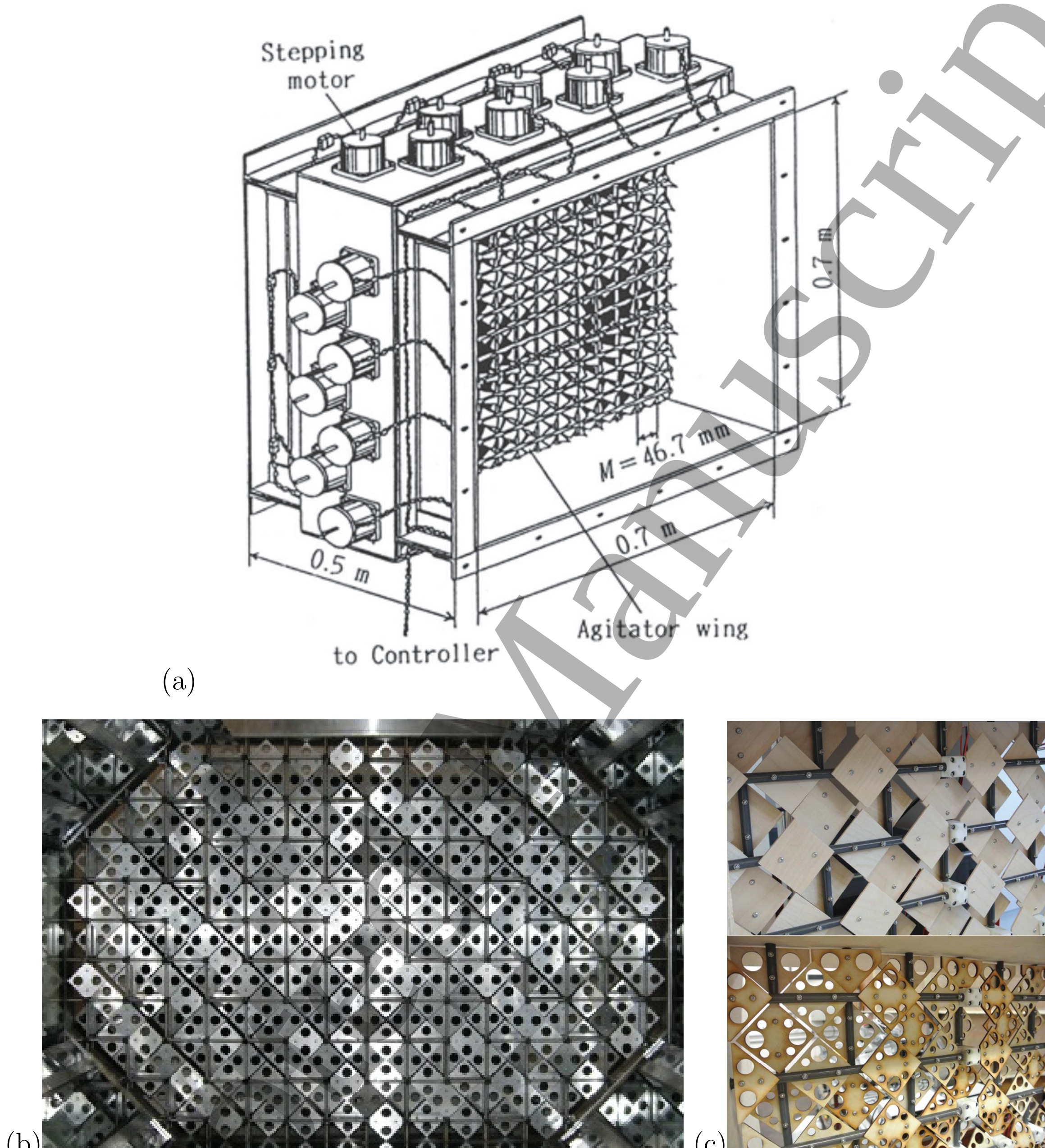

Figure 1: Active grids. (a) Schematic of the active grid developed by Makita (1991) (from Makita and Sassa (1991), with permission of Springer). (b) Active grid of Hearst and Lavoie (2015) in the University of Toronto Institute for Aerospace Studies wind tunnel (of octagonal cross-section). With permission of Springer. (c) Close-up of different winglets used by Dogan et al. (2016) in an active grid at the University of Southampton. With permission of Cambridge University Press. In (b), note that the holes in the wings were drilled to reduce their mass and inertia, but the wings were then covered with self-adhesive plastic sheets so that air could not pass through them. In (c), note the couplings connecting horizontal and vertical grid bars, to add rigidity to the grid, reduce deflection of the bars, and prevent relative motion of one bar with respect to another.

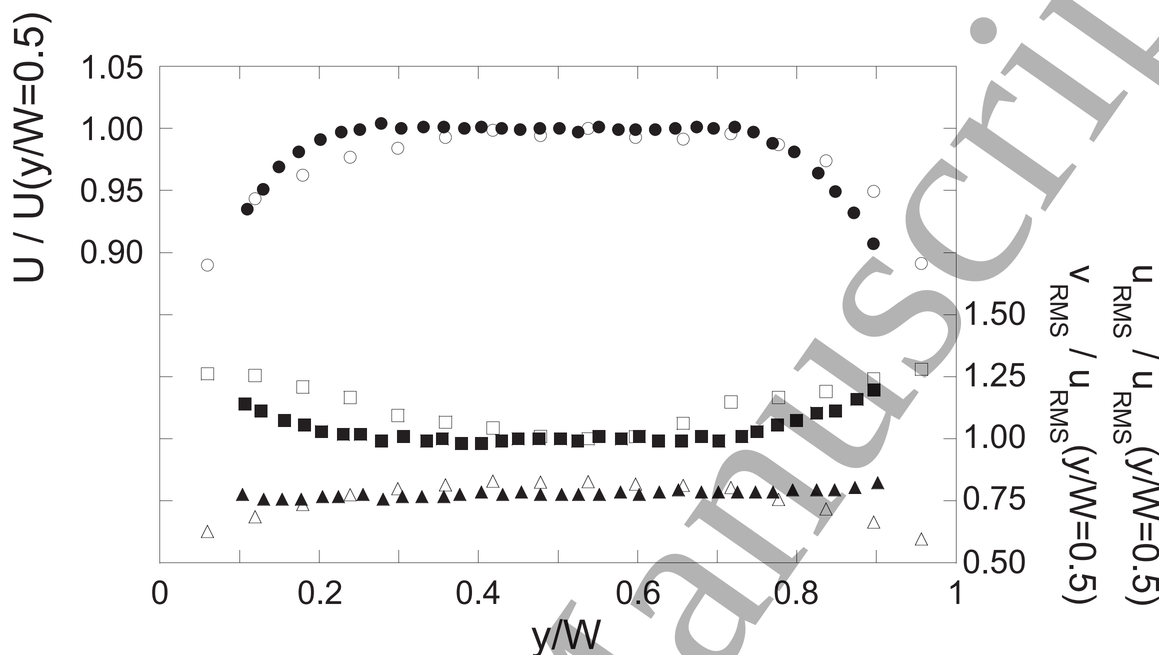

Figure 2: Transverse profiles of the mean longitudinal velocity normalized by its centreline value ($U/U(y/W = 0.5)$), and the longitudinal and transverse RMS velocity profiles normalized by the centreline value of the longitudinal RMS velocity ($u_{RMS}/u_{RMS}(y/W = 0.5)$ and $v_{RMS}/u_{RMS}(y/W = 0.5)$, respectively). Closed symbols correspond to the data of Makita (1991) ($x/M = 100$) and open symbols correspond to the data of Mydlarski and Warhaft (1996). Circles: $U/U(y/W = 0.5)$; Squares: $u_{RMS}/u_{RMS}(y/W = 0.5)$; Triangles: $v_{RMS}/u_{RMS}(y/W = 0.5)$.

the active-grid-generated turbulence slowly decayed in the downstream direction, and ii) PDFs of the scalar fluctuation were sub-Gaussian – both consequences of the scalar field being affected by the boundaries of the flow.‖ For a systematic study of PDFs of scalars within active- and passive-grid flows, see Gylfason and Warhaft (2004) (figure 5 in particular). The more delicate nature of the passive scalar field and its sensitivity to the mode of operation of the active grid will also be discussed in the next subsection.

Related to the issue of mesh lengths is the question of the boundary conditions at the interface of the active grid and a tunnel's interior walls. In general, two different approaches have been taken. Both involve the use of triangular "half-wings" and are depicted in figure 3. In figure 3(a), the half-wing is stationary and attached to the wind tunnel wall, with these static half-wings centred between grid bars. In figure 3(b), the agitator wings on a grid bar are offset by $\frac{1}{2}M$ along the length of the bar, such that there

‖ In perfectly homogeneous, isotropic turbulence with a mean scalar gradient, it has been shown that the (magnitude of the) mean scalar gradient remains constant in the downstream direction (Corrsin, 1952).

(a) (b)

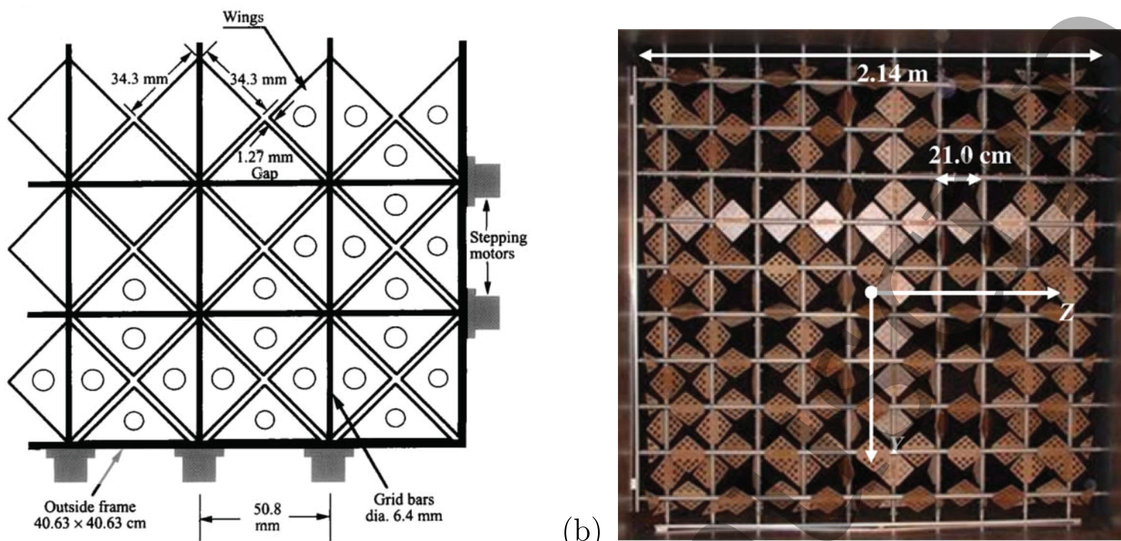

Figure 3: Near-wall, active grid boundary conditions. (a) Half-wings fixed to the interior wall (Mydlarski and Warhaft, 1996). With permission of Cambridge University Press. (b) Half-wings attached to grid rods (*e.g.* Larssen and Devenport, 2011). With permission of Springer.

is only room for a half-wing on either end of the bar. It is not clear *a priori* whether one approach has any fluid dynamical advantage over the other. To the author's knowledge, the two options have not been rigourously compared. However, what is essential to note is that, in either case, *the grid solidity of all active grids should be tuned to ensure as homogeneous of a flow as possible.* For example, in the work of Mydlarski and Warhaft (1996), the solidity of the wings adjacent to the wind tunnel walls had to be reduced (by drilling holes in near-wall winglets) due to an overly large velocity deficit close to the wall arising from the combined effects of drag from both the active-grind wings and the wind tunnel interior walls.

Another design variable that is germane to the solidity of active grids and their ultimate homogeneity is the shape of the agitator wings. The vast majority of agitator wings used in active grids built to date have been triangular in shape (or square- / diamond-shaped, given that it is easiest to make two wings on opposite sides of a grid bar out of one piece – see figure 1(c)). However, some researchers have added holes to triangular wings to improve the flow's homogeneity, as noted above, to reduce the grid's solidity, or to reduce the mass/inertia of the agitator wings. It would appear that only two groups of researchers have explicitly investigated the effects of agitator wing geometry on the turbulence generated by an active grid.

The first work to do so was that of Thormann and Meneveau (2014), who investigated the effect of wings with fractal geometries. Four wing shapes were investigated: Sierpinski triangles, space-filling squares, "Apollonian packing" fractals (i.e. a pattern of holes of decreasing diameter), and non-fractal (solid) wings. Thormann and Meneveau (2014) observed that the anisotropy associated with the aforementioned four wing geometries was 1.19, 0.77, 1.03 and 1.08, respectively. Moreover, they found that the downstream evolution of both u^2 and turbulent kinetic energy (over the range $15 \leq x/M \leq 50$) were consistent with power-law decays, with exponents between about -1.0 and -1.3, and dependent on whether or not a virtual origin was used in the least-squares regression. Thormann and Meneveau (2014) also studied the dissipation coefficient $C_\epsilon(\equiv \epsilon\ell/u^3_{RMS})$ for the four different types of active grid wings, and found that its evolution, like that of the decay exponent, was geometry-dependent but did not exhibit "systematic or monotonic trends with respect to Re_λ, component anisotropy, grid fractal dimension, or blockage ratio."

The second work to investigate the effect of agitator wing geometry was that of Hearst and Lavoie (2015), who studied the effect of wing geometry, as well as other factors. With respect to the effect of agitator wing geometry, Hearst and Lavoie (2015) investigated three wing shapes: triangular wings with holes, solid triangular wings, and solid semicircular wings. The latter were chosen as they have no sharp corners that could induce streamwise vortices with long streamwise correlations. Hearst and Lavoie (2015) found that, for the same grid-bar rotation rates, different wing shapes produced different turbulent intensities; the grid with solid triangular wings produced intensities that were notably larger than those generated by the grids with triangular wings with holes and the solid semicircular ones, both of which gave similar results. They attributed these results to the i) high ($\sim$ 100%) maximum solidity of the active grid with solid triangular wings, and ii) similar maximum solidities (79% and 78%) of the grids using triangular wings with holes and solid semicircular wings, respectively. Related to this result, Hearst and Lavoie (2015) found the effect of agitator wing geometry on Re_λ to be similar to that on the turbulence intensity (*i.e.* principally dependent on grid solidity). Lastly, Hearst and Lavoie (2015) found that the isotropy and size of the length scales characterizing the flow to be essentially independent of wing geometry.

One of the few disadvantages of active-grid-generated turbulence is a small anisotropy between the different components of the RMS velocities. As noted above, $u_{rms}/v_{rms} \approx 1.2$ for typical active grid designs and modes of operation (Makita, 1991, Mydlarski and Warhaft, 1996, Kang et al., 2003), although this value can depend on the active grid parameters (Hearst and Lavoie, 2015).¶ Fortunately, this anisotropy has been shown to be limited to the largest scales of the flow. For example, Mydlarski and Warhaft (1996) demonstrated that the i) anisotropy was maximum in a coordinate system oriented 45° to the mean flow direction, and ii) coherency spectrum of the u and v velocity fluctuations on this coordinate system fell to zero before the start of the inertial subrange – see figure 6 of Mydlarski and Warhaft (1996). This observation should be contrasted with the analogous one in shear flows, where one observes that the coherence penetrates well into the inertial subrange at similar Reynolds numbers

¶ Moreover, the axisymmetric nature of active-grid-generated turbulence is such that statistics of the turbulence are invariant to co-ordinate system rotations about the axis parallel to the mean flow (*i.e.* normal to the active grid) so that $v_{rms} \approx w_{rms}$ and $u_{rms}/v_{rms} \approx u_{rms}/w_{rms}$ (Makita and Miyamoto, 1983).

(Saddoughi and Veeravalli, 1994). In certain situations, this large-scale anisotropy is sufficiently small to not significantly affect the phenomena under study. However, should the user of an active grid need to reduce or eliminate this anisotropy, it can be done using the same approach taken to minimize the anisotropy that characterizes passive-grid turbulence. This technique generally consists of the use of a secondary contraction downstream of the grid, as first demonstrated by Comte-Bellot and Corrsin (1966). An interesting variation on this approach was employed by Larssen and Devenport (2011), who placed their active grid upstream of the wind tunnel test section, within the contraction, at a suitably chosen location therein to provide the desired contraction ratio downstream of the active grid to minimize the anisotropy. This approach is useful as it eliminates the need for a second contraction. Another approach to reduce the anisotropy was explored by Poorte and Biesheuvel (2002), who varied the orientation of the agitator wings along a given grid bar. Although they were successful in reducing the anisotropy, their approach resulted in lower Reynolds number flows, because the staggered orientation of the agitator wings had the effect of reducing the turbulence intensity of the flow given that the instantaneous solidity of the active grid became less variables, as both very low and very high grid solidities became less probable. (See Poorte and Biesheuvel (2002) for more details.)

2.2. Active grid operation

Once an active grid has been constructed, the active grid user must then consider the manner in which it is operated, *i.e.* how the grid bars are rotated. The mode of operation of the first active grids was elegantly classified by Poorte and Biesheuvel (2002) as falling into one of three categories:

(i) *synchronous mode*, in which the magnitude of the angular velocity (*i.e.* rotation rate) of each grid bar ($|\Omega|$) is constant and equal, but in which the angular velocity of adjacent grid bars have opposite signs, so as to not inject a net vorticity into the flow,

(ii) *single-random asynchronous mode (hereinafter referred to as "single-random" mode)*, in which individual grid bars will have an angular velocity of either $|\Omega|$ or $-|\Omega|$ for a randomly selected duration, after which a grid bar will change its direction of rotation (with the same angular velocity magnitude as before, but with opposite sign) for another randomly selected duration, until it changes again, and

(iii) *double-random asynchronous mode (hereinafter referred to as "double-random" mode)*, in which both the magnitude of the rotation rate of an individual grid bar, and the time interval until its next direction change, are random variables.

Mydlarski and Warhaft (1996) observed that the principal differences between the synchronous and single-random modes were that i) the former produced a lower turbulence intensity and smaller integral length scale (and thus smaller Re_λ for the same mean wind tunnel speed), and ii) the low-wavenumber, energy-containing range of the power spectral density (hereinafter referred to as the spectrum) of the velocity fluctuations was more contaminated by the grid bar rotation frequency (exhibiting a spike in the spectrum at $2|\Omega|$ – see also Poorte and Biesheuvel (2002)). However, apart from these differences, Mydlarski and Warhaft (1996) noted that the nature of the results (*e.g.* spectral slopes, PDFs, and especially results not overly dependent on the large scales of the flow) were similar when the Reynolds number was the same – an observation more rigourously tested and echoed by Hearst and Lavoie (2015).

A second active grid developed by Mydlarski and Warhaft (1998a) was built and driven by a modified single-random algorithm in which each grid bar's rotation rate was constant, but the magnitude of each bar's rotation rate was slightly different, taking on different values around a nominal value. This modification eliminated the spike from the spectrum of velocity – see their figure 4. The temperature spectrum in this mode of operation interestingly now exhibited a broad bump in the range of frequencies over which the grid bars' rotation rates were distributed, whereas it had previously been characterized by a distinct spike at a single frequency. This observation reflects the increased sensitivity of a scalar field to the mode of operation of the active grid, given that the velocity spectrum was free of spikes or other phenomena associated with the grid bar rotation rates. To the author's knowledge, no other work has been undertaken to further investigate the sensitivity of scalar fields to active grid modes of operation.

The above observations led to the proposal of the double-random mode, in which grid bar rotation rates randomly change. In this mode of operation, a grid bar begins to rotate at a given angular velocity (Ω), and continues at that rate for a time T (the so-called "cruise time"). The grid bar then reverses its direction and rotates at a new (randomly selected) angular velocity for a new (randomly selected) cruise time. Although a multitude of possible ways exist for determining the random variables Ω and T, a preferred way has been to select their values from uniform probability distributions with specified mean values of rotation rate and cruise time ($\overline{\Omega}$ and $\overline{T}$) and maximum deviations (ω and t) from the mean that bound the distribution (Poorte and Biesheuvel, 2002, Larssen and Devenport, 2011, Hearst and Lavoie, 2015). Independent of the smallest details regarding the algorithms used to calculate Ω and T, the evidence clearly suggests that *the double-random mode of operation is the preferred mode of operation for active grids designed to generate homogeneous isotropic turbulence.* In all cases, however, it is advised that, if possible, $\overline{\Omega}$ be chosen to be smaller than the inverse of the integral time scale of the flow, so as to minimize any effect of the grid on the inertial range dynamics.

For further details on the possible operation modes of active grids, the reader is referred to the extensive parameter studies on this topic by Larssen and Devenport (2011) and Hearst and Lavoie (2015). Larssen and Devenport (2011) investigated the effect of downstream distance (x/M), grid Reynolds number ($Re_M \equiv UM/\nu$), grid bar Rossby number ($Ro \equiv U/(M\overline{\Omega})$), average number of grid bar rotations between direction changes ($\overline{T}\,\overline{\Omega}$), normalized maximum deviation of cruise times ($t/\overline{T}$), and normalized maximum deviation of rotation rates ($\omega/\overline{\Omega}$) on various properties of the flow generated by an active grid. Their principal conclusions were that Re_M and Ro were the two most important parameters in controlling the flow and that the turbulence intensity, ℓ, ϵ and Re_λ all increased with increasing Re_M and Ro. They specifically noted a strong tendency towards larger ℓ as Ro increased, correlating lower rotation rates with larger flow structures. Larssen and Devenport (2011) also observed an increasing trend between Re_λ and Re_M, as would be expected, albeit with scatter associated with the dependence of λ on the different Rossby numbers in their experiments. (See figure 4(a), in which the passive grid data of Larssen and Devenport (2011) is also plotted. Note the substantial increase in Re_λ achieved by use of an active grid.)

Hearst and Lavoie (2015) studied a similar set of parameters on the turbulence generated downstream of their active grid, and also included the effect of agitator wing geometry, and a total of eight permutations of active grid operational modes. They too concluded that Re_M and Ro were two of the three most important parameters dictating the flow generated by the active grid. (The third one being wing geometry.) Specifically, they noted that the turbulence intensity increased with Ro, up to a maximum value of 50, after which increasing Ro no longer had a noticeable effect – see figure 4(b). They also made a similar observation for the Rossby number dependence of Re_λ. Furthermore, they concluded that the wing rotational period ($T \pm t$) did not measurably influence the turbulence produced by their active grid in their experiments, in which the rotations period varied from 2.11 ± 2.07s to 7.78 ± 2.69s. Similarly, they found the angular acceleration of the grid bars between direction changes to not have a measurable effect on the flow. They also found no difference between the use of Gaussian and uniform probability distributions for their random variables (*e.g.* Ω, T). (Knowing which variables are unimportant is also of great benefit!) With respect to an important practical aspect, Hearst and Lavoie (2015) measured the normalized pressure drop across active grids for a variety of configurations. Their data should be useful to researchers needing to size a blower for a wind tunnel in which an active grid will be installed, as predicting the pressure drop across an active grid is not as straightforward as it is for a passive one, for which correlations for pressure drop through meshes can be readily employed.

Lastly, note that other modes of active grid operation have been developed, with the aim of generating customized flows, other than homogeneous isotropic turbulence. This topic is addressed the next section.

3. Flow customization using active grids

Although the active grid was invented to generate high-Reynolds-number, homogeneous, isotropic turbulence, a novel trend emerging in the scientific literature is the use of active grids for the generation of new turbulent flows with specific characteristics, different from those of homogeneous, isotropic flows.

The most notable example is the customization of the operating methods of active grids to emulate the turbulence of the atmospheric boundary layer, which is neither

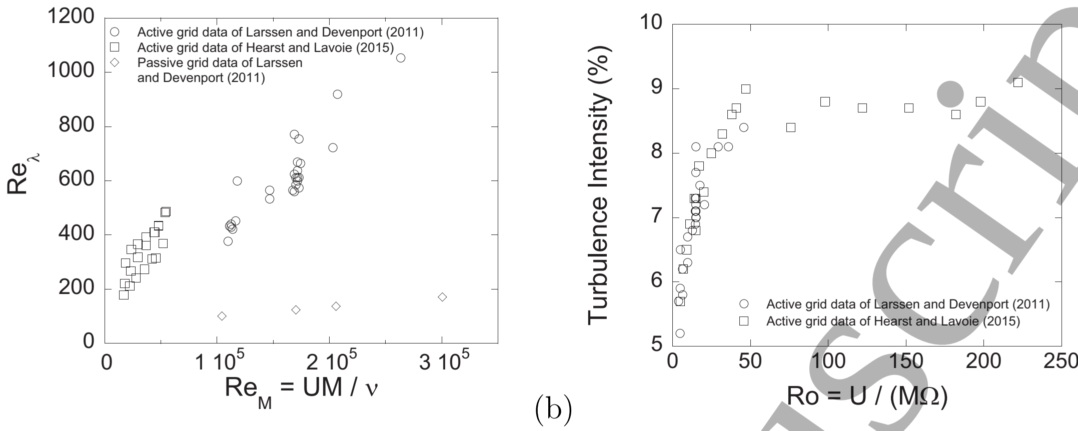

Figure 4: Effect of active grid operating parameters on the resulting flow. (a) Re_λ as a function of Re_M. (b) Turbulence intensity as a function of grid Rossby number. ◯: Active grid data of Larssen and Devenport (2011). □: Active grid data of Hearst and Lavoie (2015). ⋄: Passive grid data of Larssen and Devenport (2011). The data were selected from the test cases of Larssen and Devenport (2011) and Hearst and Lavoie (2015) that were comparable. Cases 1-30 of Larssen and Devenport (2011) used. All were measured at $x/M = 37.3$. Cases U1b - U21b of Hearst and Lavoie (2015) used. All were measured at $x/M = 41$ and used solid triangular agitator wings, as were also used for all cases in Larssen and Devenport (2011). Note that Larssen and Devenport (2011) and Hearst and Lavoie (2015) use marginally different definitions of the turbulence intensity, which are identical in isotropic flows, so the difference should not be significant herein.

homogeneous nor isotropic, nor Gaussian in nature. To this end, Cekli and van de Water (2010) attempted to simulate an atmospheric boundary layer using an active grid in which the angle of each grid bar was known and controllable. They accomplished this by tuning the solidity profile of the active grid, dictating the appropriate angles of each grid bar. The characteristics of the flow were then achieved by controlling the amplitude and frequency of the oscillations of the grid bars about these values. (Cekli and van de Water (2010) were also able to generate homogeneous turbulent shear flow in the same manner.) Knebel et al. (2011) and Good and Warhaft (2011) focussed on using active grids to generate intermittent velocity fields to model those that occur in the atmosphere. Like Cekli and van de Water (2010), Knebel et al. (2011) accomplished this by employing an active grid in which the angle of each grid bar could be precisely controlled. By specification of the PDFs of the grid bar angles, they were able to generate intermittent flows downstream of the active grid that also exhibited large (> 25%) turbulence intensities. Good and Warhaft (2011) generated inhomogeneous, intermittent flows by removing the center rows of agitators in an active grid to generate a complex wind field that was typical of those encountered by wind turbines.

Van de Water and co-workers have also undertaken further investigations pertaining to the tailoring of active-grid-generated flows. Cekli et al. (2010) observed a periodic resonant response of the dissipation rate of turbulent kinetic energy to the synchronous forcing of the grid bars. Cekli et al. (2015) studied the relationship between the statistical properties of model-turbulence signals used to control the grid bar angular positions and the resulting turbulence generated by the active grid. They concluded that both the distribution and correlation of the signals used to control the grid bar positions were important and could substantially change the generated flow. Peinke and co-workers have used their active grid, which also has control of individual bar positions, to generate multi-scale flows in which the local solidity (but not the total one) changed in space and time. They found that the local distribution of the grid solidity had a strong influence on the flow it generated (Weitemeyer et al., 2013). Heißelmann et al. (2016) investigated the effect of two tailored (sinusoidal and intermittent) grid protocols on pressure distributions over an airfoil. In these cases, the tuning of flows was achieved by control of individual grid bars.

In summary, progress in customizing flows is expected to evolve with advances in active grids. For example, the active grid discussed in Bodenschatz et al. (2014) has 129 degrees of freedom, as the angle of each agitator wing can be controlled independently. As has been the case with the development of other technologies, once active grids became sufficiently accessible, their builders then envisaged other uses and developed new ways to address these needs. It will therefore be of interest to observe how this trend continues and to note what other functions active grids will take on in the future.

4. Scientific accomplishments arising from the use of active grids

Having discussed the details pertaining to generation of high-Reynolds-number flows by means of active grids, it is now of interest to consider the scientific accomplishments that have been achieved thanks to their invention. The majority of accomplishments to be reviewed will be physical ones, pertaining to advances in our understanding of fluid dynamics; however, some technical advances will also be discussed.

It is now clear that the active grid has played a large role in the study of homogeneous, isotropic turbulence (*e.g.* Makita, 1991, Mydlarski and Warhaft, 1996, Kang et al., 2003). Moreover, it has also played an important role in advancing our understanding of the Kolomogorov theory of turbulence (Kolmogorov, 1941a,b), for two reasons. Firstly, given that Kolmogorov theory is posed in the limit of infinite Reynolds numbers, analyzing it at Reynolds numbers characteristic of passive grids was somewhat unsuitable, given the inherently low Reynolds numbers generally associated with passive grid turbulence. Active grids have substantially rectified this limitation, having achieved turbulence Reynolds numbers of $Re_\lambda \sim \mathcal{O}(10^4)$. Secondly, given that the $Re_\lambda \to \infty$ limit of Kolmogorov theory is an asymptotic one, it is therefore of interest to study the evolution of turbulent flows with Reynolds number. This latter ability is one for which active grids excel (Mydlarski and Warhaft, 1996, Larssen and Devenport, 2011, Hearst and Lavoie, 2015).

The ability of active grids to generate high-Reynolds-number turbulence has also been used to investigate the structure of fundamental turbulent flows other than homogeneous, isotropic turbulence. By using active grids in conjunction with other fluid dynamical apparatus, researchers have been able to study homogeneous turbulent shear flow (Shen and Warhaft, 2000, 2002, Warhaft and Shen, 2002, Isaza et al., 2009) and investigate the tendency of this anisotropic flow to achieve a state of small-scale (local) isotropy at high Reynolds numbers. Even though much higher Reynolds numbers have been achieved using active grids, there are still certain questions to be resolved, such as the interpretation of the differences in the evolution of statistics at third, fifth and seventh orders (Shen and Warhaft, 2000). In any case, it would seem that anisotropies observed in homogeneous turbulent shear flow, albeit non-negligible, are nevertheless smaller than those measured for passive scalar fields with a linear mean temperature gradient advected by homogeneous, isotropic turbulence (Mydlarski and Warhaft, 1998a,b).

Another fundamental class of flows studied at higher Reynolds numbers by means of active grids is inhomogeneous shearless flows (*i.e.* turbulent flows with uniform mean velocities – and therefore without mean shear – but with inhomogeneous turbulent fluctuation fields). For example, Kang and Meneveau (2008) investigated the evolution of a shearless mixing layer between two regions of homogeneous isotropic turbulence with different turbulence intensities (but the same mean velocity) using an active grid. This flow was generated by removing the agitator wings from one half of the grid's cross-section. Subsequently, Thormann and Meneveau (2015) studied a flow with a uniform mean velocity, but a transverse, linear gradient of turbulent kinetic energy. This latter flow was generated with an active grid that decreased in solidity / wing-size in the direction of decreasing turbulent kinetic energy. (See figure 5, below.) Such modifications to active grids demonstrate their flexibility in generating different high-Reynolds-number flows, but are also discussed herein to inspire researchers with ideas for other novel flows / applications.

The effect of axisymmetric strain on the velocity and passive scalar fields has furthermore been investigated at much higher Reynolds numbers by Ayyalasomayajula and Warhaft (2006) and Gylfason and Warhaft (2009), respectively. In both cases, their results were also compared with the predictions of rapid distortion theory.

Active grids have also been used to complement the study of turbulent boundary layers. In particular, Brzek et al. (2009), Sharp et al. (2009), Dogan et al. (2016) investigated the effect of (homogeneous, isotropic) free-stream turbulence on the evolution of turbulent boundary layers. Such an application of active grids plays to their strengths, as active grids are capable of generating turbulent flows of i) varying, and ii) high turbulent intensities. Both factors are important to the study of turbulent boundary layers, as the effect of the intensity of the free-stream turbulence and the study of boundary layers under conditions of high-free-stream turbulence intensities are both important and open questions in this field.

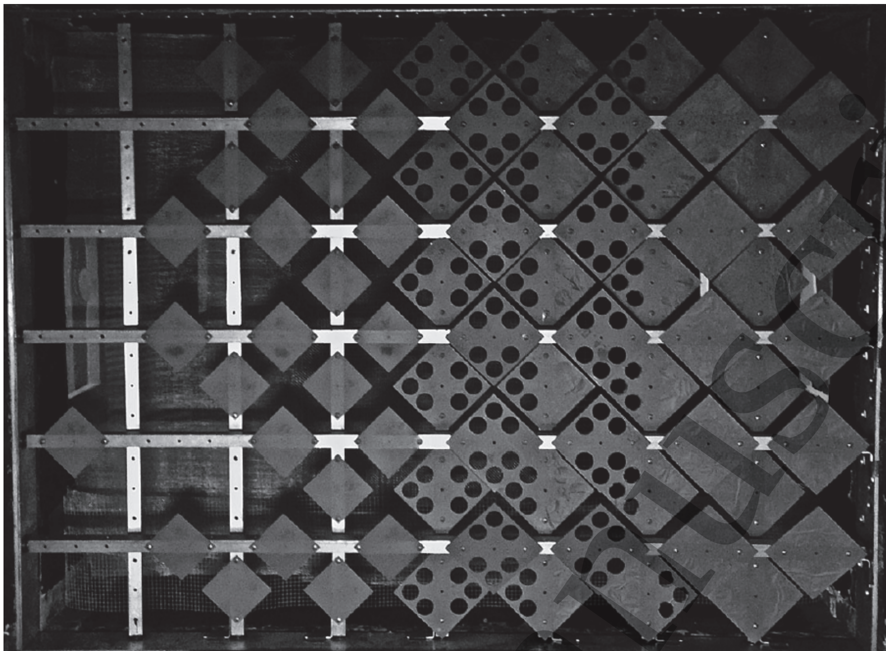

Figure 5: Active grid of Thormann and Meneveau (2015) used to generate a shearless mixing layer with a linear gradient of turbulent kinetic energy. With permission of Taylor & Francis Ltd. (*http://www.tandfonline.com/*).

Given an active grid's ability to generate high-Re_λ flows in a laboratory-sized wind tunnel, they have also been used to emulate atmospheric boundary layer turbulence, as discussed in §3. (Note that $Re_\lambda \sim \mathcal{O}(10^3)$, which is achievable using active grids, corresponds to the turbulent Reynolds numbers of the atmosphere on a weakly turbulent day (Bradley et al., 1981).) For example, active-grid turbulence has been used to model dispersion of a gas in the atmospheric boundary layer (Michioka et al., 2011); study the effects of free-stream turbulence on aerodynamic loads for low-aspect-ratio flat-plate wings (Sytsma and Ukeiley, 2013); and model the effect of atmospheric turbulence on wind turbines (Cal et al., 2010, Wachter et al., 2012, Maldonado et al., 2015), with the intention of further understanding the effects of turbulence on wind turbine aerodynamics and their associated energy conversion processes. An important issue in these studies is the intermittent nature of the atmospheric turbulence, which has important implications to wind turbine fluid dynamics. As previously noted, active grids readily lend themselves to generating such intermittent flows (Good and Warhaft, 2011, Knebel et al., 2011). Active grids can also conceivably be used to model wind loads and other atmospheric effects on buildings and structures. Extension of the work of Hearst et al. (2016), who studied the effect of (active-grid-generated) turbulence on a wall-mounted cube can be applied and/or extended to the study of the flow around buildings.

Given the advances in imaging technologies in the last 2 decades, the study of Lagrangian particle tracking within turbulent flows has rapidly advanced. And because active grids have the capacity to generate high-Reynolds-number flows, they have played a large role in this field. Moreover, this research has also been motivated in part by another atmospheric phenomena – namely the behaviour of water droplets in the atmosphere and their relationship to cloud formation, which clearly is best undertaken at high Reynolds numbers. To this end, multiple studies have been undertaken on the motion of inertial (heavy) particles within turbulent flows. Ayyalasomayajula and Warhaft (2006), Saw et al. (2008), Warhaft (2009), Siebert et al. (2010), Saw et al. (2012), Obligado et al. (2014, 2015) all examined the evolution of inertial particles (water droplets) in high-Reynolds-number, homogeneous, isotropic turbulent air flow generated by an active grid. On a related subject, more closely related to cloud formation, Gerashchenko et al. (2011), Good et al. (2012) and Gerashchenko and Warhaft (2013) have studied the entrainment of water droplets across shearless turbulent/non-turbulent (TNTI) and shearless turbulent/turbulent (TTI) interfaces in flows generated by active grids.

Studies pertaining to light particles in turbulent flows (*e.g.* air bubbles in water) have also been undertaken. These experiments were undertaken in a water tunnel with a vertical test section, using an active grid to generate the turbulence (Poorte and Biesheuvel, 2002, Prakash et al., 2012).

An active grid in a (horizontal) water tunnel was used in a novel fashion to study free-surface turbulence. To this end, Savelsberg and van de Water (2008, 2009) examined the properties of a (deformed) free surface of a water flow, relating them to the underlying velocity field that was generated by an active grid used in an open channel flow.

Finally, active grids have also inspired researchers to develop other experimental methods that overcame other limitations in existing experimental methods in fluid dynamics. The most prominent of these would be the development of Random Jet Arrays (RJAs, Variano et al. (2004), Variano and Cowen (2008)), which are novel devices that generate effectively zero-mean-flow, homogeneous, isotropic turbulence. Whereas such a class of flows were previously best generated by oscillating grids (De Silva and Fernando, 1994), the development of RJAs has enabled the generation of such flows in a much simpler fashion, requiring only an array of pumps, and no large, moving grids (some $\mathcal{O}(1m \times 1m)$ in size) needing to be oscillated back and forth multiple times per second. RJAs function by randomly turning on and off individual pumps within an array of pumps, which have their intakes in the same reservoir as the one into which the pumps eject their fluid (generally water). Far enough away from an array, the randomly firing jets emitted from the pumps, and their respective return flows to the pumps, mix and result in a quasi-homogeneous, isotropic turbulence with zero-mean flow. This is another variation of decaying homogeneous, isotropic turbulence and, as such, is a flow of fundamental importance to fluid dynamicists. But the conception of the RJA, in which an array (or grid) of pumps operates randomly, was clearly "inspired by the extremely successful active wind tunnel grid" (Variano et al., 2004). Its development has inspired the construction of others (see Asher and Litchendorf, 2009, Bellani and

Variano, 2013, Khorsandi et al., 2013, Pérez-Alvarado et al., 2016, Carter et al., 2016), and it can be readily argued that RJAs will replace oscillating-grid turbulence in the generation of zero-mean-flow homogeneous, isotropic turbulence.

Other researchers have also developed novel experimental technologies inspired by active grids. For example, Verbeek et al. (2013) developed a compact active grid, with one stationary disk and another rotating one, to enhance the level of turbulence in pipe flows, with potential applications to flows in premixed burners. Following an analogous approach, Odier et al. (2014) developed a modified active grid consisting of 4 propellers with perforated blades used in the study of entrainment and mixing of wall-bounded gravity currents to increase the intensity of the turbulence in the currents.

To summarize, active grids can be used in a variety of fashions to study many different phenomena. In certain cases, "fundamental" flows are generated with large Reynolds numbers by means of an active grid to investigate phenomena in new flow regimes. In other cases, active grids are used to generate novel flows that could not be studied otherwise. It is hoped that the above summary furthers our understanding of the multiplicity of phenomena governed by turbulent flows that have benefitted from the use of active grids. However, note that the above list and categorizations should not be considered as being universal and/or complete. For example, active grids have also been used to: investigate the effect of turbulence on aerodynamic noise generation to simulate real road conditions in studies of vehicle aerodynamics (Iida et al., 2005); study the behaviour of piezoelectric-based energy harvesters in grid-generated turbulence (Danesh-Yazdi et al., 2015); develop a facility for the study of the effect of atmospheric turbulence on insect, bird and micro-aerial-vehicle flight (Hart et al., 2016); investigate the contribution of turbulence to the evaporation rate of fuel droplets (Marti et al., 2017).

5. Concluding remarks

In conclusion, active grids have had a major impact on the study of turbulence by experimental means, as they have allowed researchers to study flows in standard wind (or water) tunnels, that could have never been achieved prior to the invention of such grids. Without active grids, experimental turbulence research would have suffered, as many experiments might continue to be undertaken at Reynolds numbers too low to extract useful results that could be compared with i) the fundamental theories of turbulence, or ii) actual industrial or environmental flows, which occur at higher Reynolds numbers. It is also worth remarking that the ingenuity demonstrated by Makita and co-workers in inventing the active grid should not be taken for granted. There have been many advances in the study of turbulence over the last half century: new velocimetry methods, massive increases in computational resources making increasingly complex simulations feasible, improved digital imaging systems (enabling Lagrangian measurements to become practical), *etc.* These techniques, however, have been made possible due to technological innovations. With no denigration of the aforementioned advances being intended, the scientific progress that has been effected by the active grid would probably not have occurred without the intellectual innovation of its inventor. The technology behind an active grid has existed since the era of the seminal paper of Comte-Bellot and Corrsin (1966), if not earlier. Yet a successful active grid was not realized until decades of studying passive grid turbulence had passed. It is in this context that the active grid can best serve as inspiration to fluid dynamicists, and especially experimentalists. Those of us who have chosen to devote our careers to the study of turbulent flows have chosen a stimulating, but difficult path. However, if further relatively simple, elegant and creative innovations like the active grid can be developed, the future for progress in this challenging field will be notably brighter.

Acknowledgements

It was my sincere pleasure to write this review. The work of Professor Hideharu Makita on active grids had a significant impact on both my doctoral studies and subsequent career – so much so that had the work of Makita (1991) not been published, my career would have certainly taken a different path. I hope that Professor Makita accepts this review as a token of my appreciation of the great influence he has had on me.

I am also indebted to Professor Zellman Warhaft, who immediately seized the important implications and applications of active-grid-generated turbulence, and who, under his generous and wise mentorship, gave me the opportunity to work in this novel area as part of my doctoral studies. I would also be remiss in not acknowledging (the late) Mr. Edward Jordan, a gentleman and master craftsman, who expertly built the two active grids used at Cornell University. Last but not least, I would like to recognize the initial work of my colleague, Professor Chenning Tong, who performed preliminary experiments on active grids while also attending Cornell University.

This work was funded by the Natural Sciences and Engineering Research Council of Canada (grant number NSERC RGPIN 217184).

References

Asher, W. and Litchendorf, T. (2009). Visualizing near-surface concentration fluctuations using laser-induced fluorescence, *Exp. Fluids* **46**(2): 243–253.

Ayyalasomayajula, S. and Warhaft, Z. (2006). Nonlinear interactions in strained axisymmetric high-Reynolds-number turbulence, *J. Fluid Mech.* **566**: 273–307.

Bellani, G. and Variano, E. (2013). Homogeneity and isotropy in a laboratory turbulent flow, *Exp. Fluids* **55**(1): 1646.

Bodenschatz, E., Bewley, G. P., Nobach, H., Sinhuber, M. and Xu, H. (2014). Variable density turbulence tunnel facility, *Rev. Sci. Instrum.* **85**(9): 093908.

Bradley, E., Antonia, R. and Chambers, A. (1981). Turbulence Reynolds number and the turbulent kinetic energy balance in the atmospheric surface layer, *Bound.-Layer Meteor.* **21**(2): 183–197.

Brzek, B., Torres-Nieves, S., Lebrón, J., Cal, R., Meneveau, C. and Castillo, L. (2009). Effects of free-stream turbulence on rough surface turbulent boundary layers, *J. Fluid Mech.* **635**: 207–243.

Cal, R. B., Lebrón, J., Castillo, L., Kang, H. S. and Meneveau, C. (2010). Experimental study of the horizontally averaged flow structure in a model wind-turbine array boundary layer, *J. Renew. Sustain. Ener.* **2**(1): 013106.

Carter, D., Petersen, A., Amili, O. and Coletti, F. (2016). Generating and controlling homogeneous air turbulence using random jet arrays, *Exp. Fluids* **57**(12): 189.

Cekli, H. E., Joosten, R. and van de Water, W. (2015). Stirring turbulence with turbulence, *Phys. Fluids* **27**(12): 125107.

Cekli, H. E., Tipton, C. and van de Water, W. (2010). Resonant enhancement of turbulent energy dissipation, *Phys. Rev. Lett.* **105**(4): 044503.

Cekli, H. E. and van de Water, W. (2010). Tailoring turbulence with an active grid, *Exp. Fluids* **49**(2): 409–416.

Comte-Bellot, G. and Corrsin, S. (1966). The use of a contraction to improve the isotropy of grid-generated turbulence, *J. Fluid Mech.* **25**(4): 657–682.

Comte-Bellot, G. and Corrsin, S. (1971). Simple eulerian time correlation of full-and narrow-band velocity signals in grid-generated, isotropic turbulence, *J. Fluid Mech.* **48**(2): 273–337.

Corrsin, S. (1952). Heat transfer in isotropic turbulence, *J. Appl. Phys.* **23**(1): 113–118.

Danesh-Yazdi, A. H., Goushcha, O., Elvin, N. and Andreopoulos, Y. (2015). Fluidic energy harvesting beams in grid turbulence, *Exp. Fluids* **56**(8): 161.

De Silva, I. and Fernando, H. (1994). Oscillating grids as a source of nearly isotropic turbulence, *Phys. Fluids* **6**(7): 2455–2464.

Dogan, E., Hanson, R. E. and Ganapathisubramani, B. (2016). Interactions of large-scale free-stream turbulence with turbulent boundary layers, *J. Fluid Mech.* **802**: 79–107.

Gad-el Hak, M. and Corrsin, S. (1974). Measurements of the nearly isotropic turbulence behind a uniform jet grid, *J. Fluid Mech.* **62**(1): 115–143.

Gerashchenko, S., Good, G. and Warhaft, Z. (2011). Entrainment and mixing of water droplets across a shearless turbulent interface with and without gravitational effects, *J. Fluid Mech.* **668**: 293–303.

Gerashchenko, S. and Warhaft, Z. (2013). Conditional entrainment statistics of inertial particles across shearless turbulent interfaces, *Exp. Fluids* **54**(12): 105031.

Good, G. H., Gerashchenko, S. and Warhaft, Z. (2012). Intermittency and inertial particle entrainment at a turbulent interface: The effect of the large-scale eddies, *J. Fluid Mech.* **694**: 371–398.

Good, G. H. and Warhaft, Z. (2011). On the probability distribution function of the velocity field and its derivative in multi-scale turbulence, *Phys. Fluids* **23**(9): 095106.

Gylfason, A. and Warhaft, Z. (2004). On higher order passive scalar structure functions in grid turbulence, *Phys. Fluids* **16**(11): 4012–4019.

Gylfason, A. and Warhaft, Z. (2009). Effects of axisymmetric strain on a passive scalar field: Modelling and experiment, *J. Fluid Mech.* **628**: 339–356.

Hart, A., Sytsma, M. and Ukeiley, L. (2016). An aerodynamic characterization facility for micro air vehicle research, *Int. J. Micro Air Veh.* **8**(2): 79–91.

Hearst, R. J., Gomit, G. and Ganapathisubramani, B. (2016). Effect of turbulence on the wake of a wall-mounted cube, *J. Fluid Mech.* **804**: 513–530.

Hearst, R. J. and Lavoie, P. (2015). The effect of active grid initial conditions on high Reynolds number turbulence, *Exp. Fluids* **56**(10): 185.

Heißelmann, H., Peinke, J. and Hölling, M. (2016). Experimental airfoil characterization under tailored turbulent conditions, *J. Phys.: Conf. Ser.* **753**(7): 072020.

Iida, A., Morita, K. and Tanida, H. (2005). Effects of turbulence on aerodynamic noise generation, *Forum Acusticum Budapest 2005: 4th European Congress on Acustics*, pp. 953–958.

Isaza, J. C., Salazar, R. and Warhaft, Z. (2014). On grid-generated turbulence in the near- and far field regions, *J. Fluid Mech.* **753**: 402–426.

Isaza, J. C., Warhaft, Z. and Collins, L. R. (2009). Experimental investigation of the large-scale velocity statistics in homogeneous turbulent shear flow, *Phys. Fluids* **21**(6): 065105.

Kang, H. S., Chester, S. and Meneveau, C. (2003). Decaying turbulence in an active-grid-generated flow and comparisons with large-eddy simulation, *J. Fluid Mech.* (480): 129–160.

Kang, H. S. and Meneveau, C. (2008). Experimental study of an active grid-generated shearless mixing layer and comparisons with large-eddy simulation, *Phys. Fluids* **20**(12): 125102.

Khorsandi, B., Gaskin, S. and Mydlarski, L. (2013). Effect of background turbulence on an axisymmetric turbulent jet, *J. Fluid Mech.* **736**: 250–286.

Kistler, A. L. and Vrebalovich, T. (1966). Grid turbulence at large Reynolds numbers, *J. Fluid Mech.* **26**(1): 37–47.

Knebel, P., Kittel, A. and Peinke, J. (2011). Atmospheric wind field conditions generated by active grids, *Exp. Fluids* **51**(2): 471–481.

Kolmogorov, A. (1941a). The local structure of turbulence in incompressible viscous fluid for very large Reynolds numbers, *Dolk. Akad Nauk SSSR* **30**: 301–305.

Kolmogorov, A. (1941b). Dissipation of energy in locally isotropic turbulence, *Dolk. Akad Nauk SSSR* **32**: 16–18.

Larssen, J. V. and Devenport, W. J. (2011). On the generation of large-scale homogeneous turbulence, *Exp. Fluids* **50**(5): 1207–1223.

Lavoie, P., Djenidi, L. and Antonia, R. A. (2007). Effects of initial conditions in decaying turbulence generated by passive grids, *J. Fluid Mech.* **585**: 395–420.

Lee, S., Djenidi, L. and Antonia, R. A. (2014). Empirical correlations for slightly heated decaying passive-grid turbulence, *Heat Transfer Eng.* **35**(16-17): 1482–1490.

Ling, S. and Wan, C. (1972). Decay of isotropic turbulence generated by a mechanically agitated grid, *Phys. Fluids* **15**(8): 1363–1369.

Makita, H. (1991). Realization of a large-scale turbulence field in a small wind tunnel, *Fluid Dyn. Res.* **8**(1-4): 53–64.

Makita, H., Iida, A. and Sassa, K. (1988). Evaluation of the characteristic features of a large-scale turbulence field : 4th report, on turbulence Reynolds number and Kolmogorov universal constant, *Trans. JSME (B)* **54**(505): 2333–2339.

Makita, H., Iwasaki, T., Ida, A. and Sassa, K. (1988). Evaluation of the characteristic features of a large-scale turbulence field : 3rd report, on the scales and the anisotropy of the turbulent flow field, *Trans. JSME (B)* **54**(497): 37–44.

Makita, H. and Miyamoto, S. (1983). *Proc. 2nd Asian Conference on Fluid Mechanics, Beijing, China*, p. 101.

Makita, H. and Sassa, K. (1991). Active turbulence generation in a laboratory wind tunnel, *in* A. Johansson and P. Alfredsson (eds), *Advances in Turbulence 3, Springer-Verlag Berlin*, pp. 497–505.

Makita, H., Sassa, K. and Iida, A. (1989). *Proc. 4th Asian Conference on Fluid Mechanics, Hong Kong*, p. G85.

Makita, H., Sassa, K., Iwasaki, T. and Iida, A. (1987a). Evaluation of the characteristics features of a large-scale turbulence field (1st report, performance of the turbulence generator), *Trans. JSME (B)* **53**: 3173–3186.

Makita, H., Sassa, K., Iwasaki, T. and Iida, A. (1987b). Evaluation of thebcharacteristic features of a large-scale turbulence field : 2nd report, on the statistical quantities of the turbulence, *Trans. JSME (B)* **53**(495): 3180–3186.

Maldonado, V., Castillo, L., Thormann, A. and Meneveau, C. (2015). The role of free stream turbulence with large integral scale on the aerodynamic performance of an experimental low Reynolds number s809 wind turbine blade, *J. Wind Eng. Ind. Aero.* **142**: 246–257.

Marti, F., Martinez, O., Mazo, D., Garman, J. and Dunn-Rankin, D. (2017). Evaporation of a droplet larger than the Kolmogorov length scale immersed in a relative mean flow, *Int. J. Multiph. Flow* **88**: 63–68.

Michioka, T., Sato, A. and Sada, K. (2011). Wind-tunnel experiments for gas dispersion in an atmospheric boundary layer with large-scale turbulent motion, *Bound.-Layer Meteor.* **141**(1): 35–51.

Mydlarski, L. and Warhaft, Z. (1996). On the onset of high-Reynolds-number grid-generated wind tunnel turbulence, *J. Fluid Mech.* **320**: 331–368.

Mydlarski, L. and Warhaft, Z. (1998a). Passive scalar statistics in high-Péclet-number grid turbulence, *J. Fluid Mech.* **358**: 135–175.

Mydlarski, L. and Warhaft, Z. (1998b). Three-point statistics and the anisotropy of a turbulent passive scalar, *Phys. Fluids* **10**(11): 2885–2894.

Obligado, M., Cartellier, A. and Bourgoin, M. (2015). Experimental detection of superclusters of water droplets in homogeneous isotropic turbulence, *EPL Eurphys. Lett.* **112**(5): 54004.

Obligado, M., Teitelbaum, T., Cartellier, A., Mininni, P. and Bourgoin, M. (2014). Preferential concentration of heavy particles in turbulence, *J. Turbul.* **15**(5): 293–310.

Odier, P., Chen, J. and Ecke, R. E. (2014). Entrainment and mixing in a laboratory model of oceanic overflow, *J. Fluid Mech.* **746**(3): 498–535.

Pérez-Alvarado, A., Mydlarski, L. and Gaskin, S. (2016). Effect of the driving algorithm on the turbulence generated by a random jet array, *Exp. Fluids* **57**(2): 20.

Poorte, R. E. G. and Biesheuvel, A. (2002). Experiments on the motion of gas bubbles in turbulence generated by an active grid, *J. Fluid Mech.* **461**: 127–154.

Pope, S. B. (2000). *Turbulent Flows*, Cambridge University Press.

Prakash, V. N., Tagawa, Y., Calzavarini, E., Mercado, J. M., Toschi, F., Lohse, D. and Sun, C. (2012). How gravity and size affect the acceleration statistics of bubbles in turbulence, *New. J. Phys.* **14**: 105017.

Reynolds, O. (1883a). An experimental investigation of the circumstances which determine whether the motion of water shall be direct or sinuous, and of the law of resistance in parallel channels., *Proc. R. Soc* **35**(224-226): 84–99.

Reynolds, O. (1883b). An experimental investigation of the circumstances which determine whether the motion of water shall be direct or sinuous, and of the law of resistance in parallel channels, *Phil. Trans. R. Soc.* **174**: 935–982.

Saddoughi, S. and Veeravalli, S. (1994). Local isotropy in turbulent boundary layers at high Reynolds number, *J. Fluid Mech.* **268**: 333–372.

Savelsberg, R. and van de Water, W. (2008). Turbulence of a free surface, *Phys. Rev. Lett.* **100**(3): 034501.

Savelsberg, R. and van de Water, W. (2009). Experiments on free-surface turbulence, *J. Fluid Mech.* **619**: 95–125.

Saw, E. W., Shaw, R. A., Ayyalasomayajula, S., Chuang, P. Y. and Gylfason, . (2008). Inertial clustering of particles in high-Reynolds-number turbulence, *Phys. Rev. Lett.* **100**(21): 214501.

Saw, E.-W., Shaw, R. A., Salazar, J. P. L. C. and Collins, L. R. (2012). Spatial clustering of polydisperse inertial particles in turbulence: II. Comparing simulation with experiment, *New J. Phys.* **14**: 105031.

Sharp, S. N., Neuscamman, S. and Warhaft, Z. (2009). Effects of large-scale free stream turbulence on a turbulent boundary layer, *Phys. Fluids* **21**(9): 095105.

Shen, X. and Warhaft, Z. (2000). The anisotropy of the small scale structure in high Reynolds number ($r_\lambda \sim 1000$) turbulent shear flow, *Phys. Fluids* **12**(11): 2976–2989.

Shen, X. and Warhaft, Z. (2002). Longitudinal and transverse structure functions in sheared and unsheared wind-tunnel turbulence, *Phys. Fluids* **14**(1): 370–381.

Siebert, H., Gerashchenko, S., Gylfason, A., Lehmann, K., Collins, L. R., Shaw, R. A. and Warhaft, Z. (2010). Towards understanding the role of turbulence on droplets in clouds: In situ and laboratory measurements, *Atmos. Res.* **97**(4): 426–437.

Simmons, L. F. G. and Salter, C. (1934). Experimental investigation and analysis of the velocity variations in turbulent flow, *Proc. R. Soc. Lond. A Math. Phys. Sci.* **145**(854): 212–234.

Simmons, L. and Salter, C. (1938). An experimental determination of the spectrum of turbulence, *Proc. R. Soc. Lond. A Math. Phys. Sci.* **165**(A920): 0073–0089.

Stewart, R. W. and Townsend, A. A. (1951). Similarity and self-preservation in isotropic turbulence, *Proc. R. Soc. Lond. A Math. Phys. Sci.* **243**(867): 359–386.

Sytsma, M. J. and Ukeiley, L. (2013). Mean loads from wind-tunnel turbulence on low-aspect-ratio flat plates, *J. Aircraft* **50**(3): 863–870.

Tassa, Y. and Kamotani, Y. (1975). Experiments on turbulence behind a grid with jet injection in downstream and upstream direction, *Phys. Fluids* **18**(4): 411–414.

Tennekes, H. and Lumley, J. L. (1972). *A first course in turbulence*, MIT press, Cambridge, MA.

Thormann, A. and Meneveau, C. (2014). Decay of homogeneous, nearly isotropic turbulence behind active fractal grids, *Phys. Fluids* **26**(2): 025112.

Thormann, A. and Meneveau, C. (2015). Decaying turbulence in the presence of a shearless uniform kinetic energy gradient, *J. Turbul.* **16**(5): 442–459.

Variano, E., Bodenschatz, E. and Cowen, E. (2004). A random synthetic jet array driven turbulence tank, *Exp. Fluids* **37**(4): 613–615.

Variano, E. and Cowen, E. (2008). A random-jet-stirred turbulence tank, *J. Fluid Mech.* **604**: 1–32.

Verbeek, A. A., Pos, R. C., Stoffels, G. G. M., Geurts, B. J. and Van Der Meer, T. H. (2013). A compact active grid for stirring pipe flow, *Exp. Fluids* **54**(10).

Wachter, M., Heißelmann, H., Hölling, M., Morales, A., Milan, P., Mücke, T., Peinke, J., Reinke, N. and Rinn, P. (2012). The turbulent nature of the atmospheric boundary layer and its impact on the wind energy conversion process, *J. Turbul.* **13**: 1–21.

Warhaft, Z. (2009). Laboratory studies of droplets in turbulence: Towards understanding the formation of clouds, *Fluid Dyn. Res.* **41**(1): 011201.

Warhaft, Z. and Shen, X. (2002). On the higher order mixed structure functions in laboratory shear flow, *Phys. Fluids* **14**(7): 2432–2438.

Weitemeyer, S., Reinke, N., Peinke, J. and Hölling, M. (2013). Multi-scale generation of turbulence with fractal grids and an active grid, *Fluid Dyn. Res.* **45**(6).